ARTICLE

Rovibrational State-Selectivity in Photoassociation through Multi-photon Transitions

Rong Wang*, Ming-hui Qiu, Jun-ling Xiu

School of Science, Dalian Jiaotong University, Dalian 116028, China

(Dated: Received on May 6, 2014; Accepted on June 11, 2014)

The rovibrational state-selectivity in photoassociation (PA) is investigated for the ground electronic state of OH radical. The calculated results show that population can be transferred from continuum state to the target states through three-, four-, and nine-photon transitions by choosing suitable pulse parameters and initial collision energy. To control population transfer to a lower rovibrational state, a shorter pulse frequency has to be chosen and the photon number transferred to target state should be increased. In PA process, some associated OH radicals can be dissociated via intermediate and background states, which decreases the final population of the target state.

Key words: Photoassociation, Multi-photon transition, State-selectivity, Intermediate state

I. INTRODUCTION

The interaction of molecules with the laser field has long been a subject of considerable attention [1–5]. The preparation of well-defined quantum states with laser pulses is relevant to many applications, including quantum optics, optical control of chemical reactions, molecular spectroscopy, and quantum information processing. The localization of population at a selected energy level can be realized by properly designed laser fields, such as stimulated Raman adiabatic passage (STIRAP) [6–8], multiphoton excitation [9], chirped laser pulses [2], and optimal control theory (OCT) [10, 11]. These approaches are mainly used to control population transfer in the bound rovibrational states of the molecules.

Photoassociation (PA) is another effective method to yield molecules in specified quantum states [12–16]. In PA process, the external field induces a free-to-bound transition, and the two colliding atoms can form a molecule in its excited state or ground state by absorbing or emitting photons. There are mainly two approaches to create a molecule in the ground electronic state. For the first approach, the pump-dump scheme is employed and PA is achieved through dipole moment transition [17–19]. In this process, the population is transferred from continuum state to a bound level in an excited state by the pump pulse, and then transferred to a bound level in a ground state by the dump pulse. For the second approach, PA reaction only occurs in a ground state, and the molecule is formed directly through the interaction between the permanent dipole moment and the infrared pulse [20–23]. This approach has been frequently described in a one-dimensional model system. Korolkov *et al.* investigated the state-selective association in the ground state by infrared sub-picosecond pulses [24]. PA reaction for OH radicals has been studied in a thermal gas condition [25] and an environment condition [20]. Recently, Marquetand *et al.* employed the local control theory to achieve PA [26]. Their results show that the association yield is obviously reduced as the rotational freedom degree is taken into account.

The time-dependent quantum wave packet method is an important way to study the PA reaction [17, 20–22, 26]. By this way, the molecular reaction process and the time-dependent population distributions of the molecules can be described by the evolution of a wave packet on the corresponding potential energy surface. In this work, we take OH radical for an example to explore the PA process using the quantum wave packet method in a two-dimensional model. A shaped laser pulse is employed to induce the PA reaction in the ground state. For a PA process, it is difficult to control population transfer from continuum state to a lower rovibrational state by one-photon transition. In our model, population is transferred to a target bound state via multiple intermediate states, and the PA process is achieved by multiphoton transition. The transition pathways are controlled by choosing suitable pulse parameters and initial collision energy. In particular, we investigate numerically three-photon association corresponding to the target state $|11, 1\rangle$, four-photon association corresponding to the target state $|10, 0\rangle$, and nine-photon association corresponding to the target state $|7, 5\rangle$.

*Author to whom correspondence should be addressed. E-mail: wangrong@djtu.edu.cn

II. COMPUTATIONAL METHODS

In our theoretical model, the PA reaction takes place only in the ground electronic state. In the framework of the Born-Oppenheimer approximation, the reactive dynamics can be described by the time-dependent Schrödinger equation [24]

$$i\hbar\frac{\partial}{\partial t}\Psi(t)=\left[\hat{H}_{\rm mol}+\hat{W}(t)\right]\Psi(t) \tag{1}$$

where $\hat{H}_{\rm mol}$ is the Hamiltonian of the OH, and $\hat{W}(t)$ denotes the interaction between the OH and the laser pulse.

In the linearly polarized laser field, the molecular magnetic quantum number M=0 is conserved, and the two-dimensional molecular Hamiltonian can be expressed as

$$\hat{H}_{\rm mol}=-\frac{\hbar^2}{2m}\frac{\partial^2}{\partial R^2}-\frac{\hbar^2}{2mR^2}\frac{1}{\sin\theta}\frac{\partial}{\partial\theta}\left(\sin\theta\frac{\partial}{\partial\theta}\right)+\hat{V}(R) \tag{2}$$

where R is the internuclear separation, m is the reduced mass of OH. The potential energy curve $\hat{V}(R)$ for the ground electronic state is the Morse potential function, and the parameters of the function are adapted from Ref.[24].

The field-molecule interaction term $\hat{W}$ can be written as

$$\hat{W}=-\varepsilon(t)\cos\theta\mu(R) \tag{3}$$

where $\mu(R)$ is the permanent dipole moment, $\varepsilon(t)$ the electric field, and θ the angle between the molecular axis and the laser electric field axis. $\mu(R)$ is described by the function [27]

$$\mu(R)=q_0R\exp\left(-\frac{R}{R_0}\right) \tag{4}$$

where q_0=7.85 D/Å, and R_0=0.6 Å for OH bonds in H_2O molecules. The electric field $\varepsilon(t)$ can be represented by a $\sin^2$-shaped pulse

$$\varepsilon(t)=E_p\sin^2\left[\frac{\pi(t-t_0)}{\tau}\right]\cos[\omega_p(t-t_0)] \tag{5}$$

where E_p, τ, t_0, and ω_p are the electric field amplitude, duration, start time, and carrier frequency respectively.

The radial function of the initial wave for an atomic beam is described by a Gaussian wave packet [20, 26, 28]

$$\phi(R,t=0)=\left(\frac{2}{\pi a^2}\right)^{1/4}\exp\left[ik_eR-\left(\frac{R-R_e}{a}\right)^2\right] \tag{6}$$

where the initial width of the wave packet a=10a_0, the average initial distance of the two colliding atoms R_e=30a_0 (a_0 is the Bohr radius), and $\hbar k_e$ is the initial momentum. The angular wave function can be given by the Legendre polynomial $P_j(\cos\theta)$, and the initial rovibrational wave function $\Psi(R,\theta,t$=0) can be obtained by a direct product of the radial function and angular function. We assume that initial collision is s-wave scattering (orbital angular momentum **j**=0). Because the initial rotational energy is zero, the initial collision energy can be expressed as

$$E_0=\frac{\hbar^2}{2m}\left(k_e^2+\frac{1}{a^2}\right) \tag{7}$$

The Fortran routines are used to perform the propagation of the initial wave function through the split operator method [29, 30]. By projecting the total wave function $\Psi(t)$ onto the rovibrational eigenstates $|v,j\rangle$, one can compute the time-dependent population of the rovibrational levels

$$P_{v,j}(t)=|\langle v,j|\Psi(t)\rangle|^2 \tag{8}$$

The rovibrational eigenfunction $|v,j\rangle$ can be obtained by a direct product of angular eigenfunction and radial eigenfunction which is calculated by the Fourier grid Hamiltonian method [31]. The total yield of associated OH radicals can be written as

$$P_{\rm yield}(t)=\sum_v\sum_j P_{v,j}(t) \tag{9}$$

III. RESULTS AND DISCUSSION

As the resonant frequencies between the intermediate and target states are close to each other, the multiphoton transitions can take place. We have calculated all the resonant frequencies between two deferent rovibrational states to find the proper target and intermediate states for multiphoton transitions. For the transitions, $|16,1\rangle\rightarrow$ (one-photon) $\rightarrow|13,0\rangle(|13,2\rangle)\rightarrow$ (one-photon) $\rightarrow|11,1\rangle$, their one-photon resonant frequencies are similar. Therefore, these four states can be chosen as the intermediate and target states for three-photon PA reaction. The energy spacing between the initial collision energy E_0 and the eigenenergy of the first intermediate state $|16,1\rangle$ should be close to the resonant frequencies between the intermediate and target states. According to this condition, the initial collision energy is adjusted to obtain the optimal value until the target population reaches the maximal value. For the three-photon PA reaction, the optimal E_0 is 10.05 kJ/mol, and the population transfer process according to the pathway

$$\begin{aligned}&\text{Continuum state}\rightarrow(\text{transition 1})\rightarrow|16,1\rangle\rightarrow\\&\left\{\begin{array}{l}(\text{transition 2})\rightarrow|13,0\rangle\rightarrow(\text{transition 4})\\(\text{transition 3})\rightarrow|13,2\rangle\rightarrow(\text{transition 5})\end{array}\right\}\rightarrow\\&\quad|11,1\rangle\end{aligned} \tag{10}$$

DOI:10.1063/1674-0068/27/05/497-502

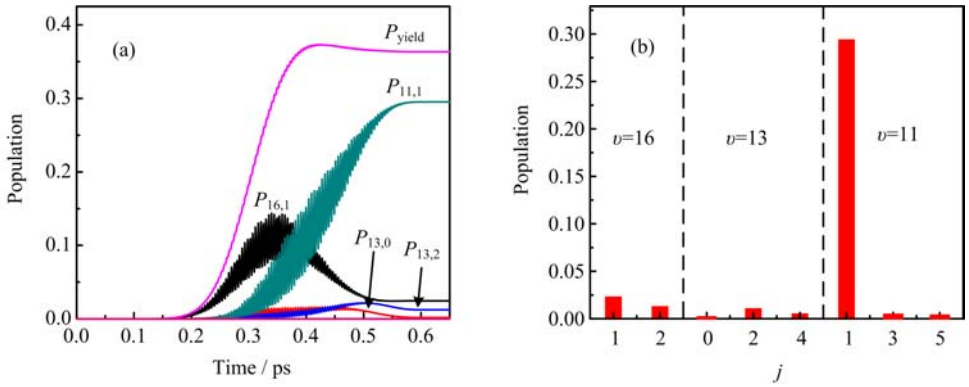

FIG. 1 The population transfer for three-photon PA reaction. (a) The total yield of associated OH radicals and the populations of the intermediate and target states. (b) The final population distributions at the end of the pulse. The laser parameters are chosen to be E_p=312.67 MV/cm, ω_p=3589.53 cm^{-1}, τ=0.605 ps, t_0=0 ps.

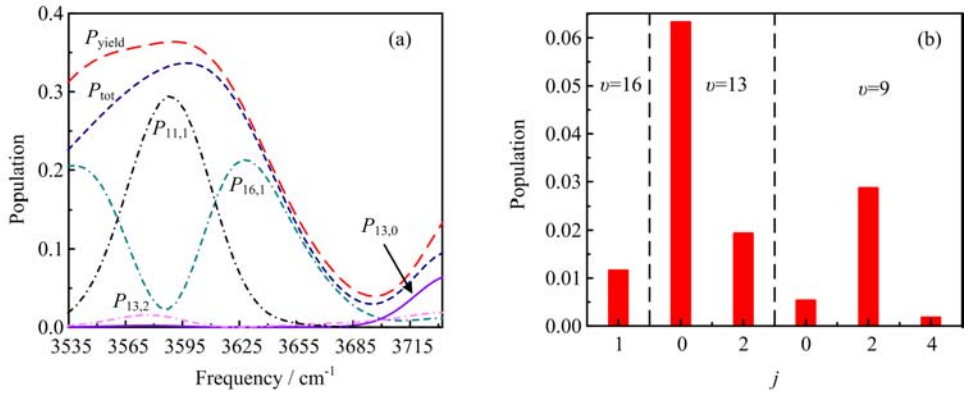

FIG. 2 (a) The population distributions for three-photon association versus the carrier frequency ω_p. (b) The final population distributuons with ω_p=3721 cm^{-1}.

The resonant frequency between the initial and target states can be given by

$$\omega_r = \frac{E_0 - E_{v,j}}{n} \tag{11}$$

where $E_{v,j}$ is the rovibrational eigenenergy for the target state, and n is the photon number. The resonant frequency ω_r is adjusted to get the optimal laser carrier frequency ω_p.

Figure 1 shows the process of three-photon PA reaction. In Fig.1(a), the population first appears in the intermediate state $|16,1\rangle$ at about 0.17 ps. When t>0.22 ps, the population $P_{16,1}$ is transferred to the target state $|11,1\rangle$ via the intermediate states $|13,0\rangle$ and $|13,2\rangle$. When the pulse is over, the target-state population reaches 0.295, and the populations of three intermediate states $|16,1\rangle$, $|13,0\rangle$, and $|13,2\rangle$ are 0.024, 0.002, and 0.012, respectively. The total yield of OH reaches 0.364, and the state-selectivity is $P_{11,1}/P_{\rm yield}$=81%. For the population curves of the intermediate and target states, the large amplitude oscillation results from the population transfer in the intermediate, target, and background states. On the contrary, a slight oscillatory behavior can be found in the curve of the total yield, which indicates that only a small amount of associated OH may be dissociated in PA process. The transition pathway (10) includes five transitions. For the transition 1 (continuum state→$|16,1\rangle$), the one-photon detuning $\triangle_{31}$ of the pulse from its resonant frequency is 32.98 cm^{-1}. The detunings for the transitions 2 and 3 are 238.05 and 181.07 cm^{-1}, respectively. Because of the transition 1 with a smaller detuning, the maximum value of population in the first intermediate state $|16,1\rangle$ is larger than those in the states $|13,0\rangle$ and $|13,2\rangle$.

Besides the transition pathway (10), the shaped pulse can induce some other transitions, such as the pathway

$$|13,2\rangle \rightarrow \left\{ \begin{array}{l} |16,3\rangle \\ |11,3\rangle \end{array} \right\} \rightarrow |13,4\rangle \rightarrow |11,5\rangle \tag{12}$$

A small amount of population can be transferred to the background states through these transitions. Figure 1(b) shows the rovibrational population distributions when the pulse is over. The populations of the background states $|16,3\rangle$, $|13,4\rangle$, $|11,3\rangle$, and $|11,5\rangle$ are 0.014, 0.008, 0.005, and 0.004, respectively. The transitions between the state $|13,2\rangle$ and the background states increase the final population in the state $|13,2\rangle$.

DOI:10.1063/1674-0068/27/05/497-502

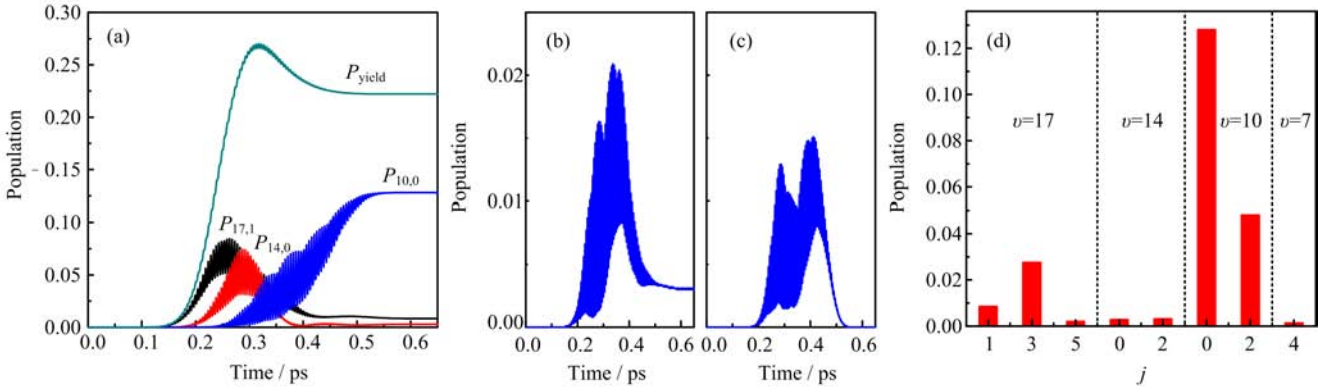

FIG. 3 The population transfer for four-photon PA reaction. (a) The total yield $P_{\rm yield}$ and the populations $P_{17,1}$, $P_{14,0}$, and $P_{10,0}$. (b) The population of the intermediate state $|14,2\rangle$. (c) The population of the intermediate state $|12,1\rangle$. (d) The final population distributions at the end of the pulse.

Thus, the final population in the state $|13,2\rangle$ is larger than that in the state $|13,0\rangle$.

The population distributions of associated OH depend on the carrier frequency ω_p, as shown in Fig.2(a). The curve $P_{\rm tot}$ is for the total population of the target and intermediate states. As the carrier frequency is turned away from the optimal frequency, the population of the target state decreases, and the population of the first intermediate state increases. When the carrier frequency ω_p<3600 cm^{-1}, the ratio $P_{\rm tot}/P_{\rm yield}$ decreases with decreasing ω_p, which indicates that more population is transferred to the background states. When ω_p>3600 cm^{-1}, the two populations for $P_{\rm tot}$ and $P_{\rm yield}$ decrease rapidly with increasing frequency. For the region 3640 cm^{-1}<ω_p<3680 cm^{-1}, the three nearly overlapping curves $P_{\rm tot}$, $P_{\rm yield}$, and $P_{16,1}$ show that most of the population stays in the state $|16,1\rangle$. When ω_p>3700 cm^{-1}, the carrier frequency ω_p is close to the four-photon resonant frequency, $(E_0-E_{9,2})/4$=3743.12 cm^{-1}, the total yield $P_{\rm yield}$ and the intermediate-state populations $P_{13,0}$ and $P_{13,2}$ are increased, and some population can be found in the state $|9,2\rangle$ in Fig.2(b).

We now present the calculated results for four-photon PA reaction in which the initial collision energy E_0 is chosen as 17.41 kJ/mol, the target state is $|10,0\rangle$, and the four intermediate states are $|17,1\rangle$, $|14,0\rangle$, $|14,2\rangle$, and $|12,1\rangle$. The pathway for the four-photon transition is as follows:

$$\begin{aligned}&\text{Continuum state} \rightarrow (\text{transition 1}) \rightarrow |17,1\rangle \rightarrow \\ &\left\{\begin{array}{l}(\text{transition 2}) \rightarrow |14,0\rangle \rightarrow (\text{transition 4}) \\ (\text{transition 3}) \rightarrow |14,2\rangle \rightarrow (\text{transition 5})\end{array}\right\} \rightarrow \\ &|12,1\rangle \rightarrow (\text{transition 6}) \rightarrow |10,0\rangle \end{aligned} \quad (13)$$

ω_p is chosen as 3379.43 cm^{-1}.

Figure 3 shows the process of four-photon PA reaction. It can be seen from Fig.3(a) that the curves for $P_{\rm yield}$ and $P_{10,0}$ appear at t=0.13 and 0.23 ps. The total yield reaches the maximum value 0.270 at t=0.32 ps and then decreases to 0.222. When the pulse is over, the populations of the four intermediate states are 0.008, 0.003, 0.003, and 0, respectively. The final population of target state is 0.128 and the state-selectivity is 58%. In four-photon PA reaction, the one-photon detuning $\triangle_{41}$ is smaller than the other detunings ($\triangle_{42}$, $\triangle_{43}$, $\triangle_{44}$, and $\triangle_{45}$), and the maximal population in the state $|17,1\rangle$ is larger than those in the states $|14,0\rangle$, $|14,2\rangle$, and $|12,1\rangle$, as shown in Figs.3 (a)−(c). It can be seen from Fig.3(d) that 0.1% of population is transferred to the state $|7,4\rangle$ through the six-photon transition.

Compared with the three-photon scheme, the four-photon scheme includes more intermediate states and transitions, which can increase the effect of background states and decrease the population of the target state. In Fig.3(d), about 5% of population, which is derived from the two transitions, $|14,2\rangle\rightarrow|12,3\rangle\rightarrow|10,2\rangle$ and $|12,1\rangle\rightarrow|10,2\rangle$, stays in the state $|10,2\rangle$, and the state-selectivity is decreased. Because the laser frequency is close to the three-photon resonant frequency (3385.53 cm^{-1}) between $|10,2\rangle$ and $|17,3\rangle$, some population in the state $|10,2\rangle$ is transferred to a higher rovibrational level $|17,3\rangle$ via the pathway

$$|10,2\rangle \rightarrow \left\{\begin{array}{lll}|12,1\rangle & \rightarrow & |14,2\rangle \\ |12,3\rangle & \rightarrow & \left\{\begin{array}{l}|14,2\rangle \\ |14,4\rangle\end{array}\right\}\end{array}\right\} \rightarrow |17,3\rangle \quad (14)$$

In Fig.3(a), the population curves for the states $|17,1\rangle$ and $|14,0\rangle$ appear one peak. For the states $|14,2\rangle$ and $|12,1\rangle$, the population curves are divided into two peaks in Figs.3 (b) and (c). The left peaks are formed by the transition from continuum state to the target state $|10,0\rangle$. When t>0.3 ps, the transition probability through the pathway (14) is increased, which increases the population in the intermediate states $|14,2\rangle$ and $|12,1\rangle$ and forms the right peaks. The population in the state $|17,3\rangle$ can be transferred to continuum state again, and the total yield of OH is decreased. It can be seen from Fig.3(a) that $P_{\rm yield}$ is decreased as t>0.3 ps.

DOI:10.1063/1674-0068/27/05/497-502

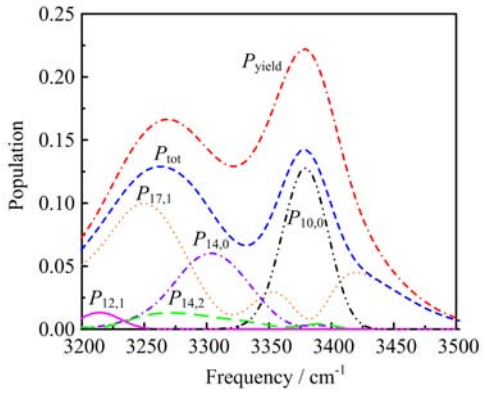

FIG. 4 The population distributions for four-photon association versus the carrier frequency ω_p.

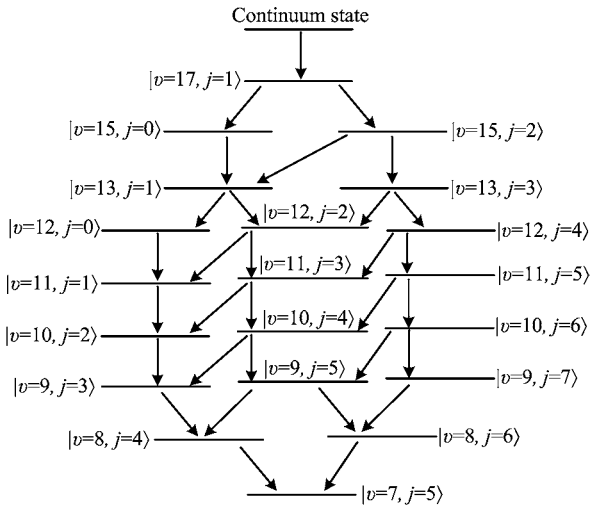

FIG. 5 Schematic diagram of nine-photon transition.

When the pulse is over, about 3% of population stays in the background state $|17, 3\rangle$ in Fig.3(d).

Figure 4 shows the total yield and the rovibrational populations for four-photon association versus the carrier frequency. When ω_p>3379 cm^{-1}, the populations $P_{\rm tot}$ and $P_{10,0}$ decrease rapidly, and the ratio $P_{\rm tot}/P_{\rm yield}$ increases with increasing frequency. As the frequency reaches 3500 cm^{-1}, the total yield $P_{\rm yield}$ is nearly zero. When ω_p=3300 cm^{-1}, the pulse frequency is close to the two-photon resonant frequency between continuum state and $|14, 0\rangle$, and population $P_{14,0}$ reaches the maximum value. As the frequency is chosen to be 3281.28 and 3224.98 cm^{-1}, corresponding to the respective resonant frequencies for two- and three-photon transition, the populations $P_{14,2}$ and $P_{12,1}$ reach nearly the maximum values. In the region 3250 cm^{-1}<ω_p<3379 cm^{-1}, the total yield $P_{\rm yield}$ decreases to 0.129, and then increases to 0.166 with decreasing frequency. As the frequency decreases from 3250 cm^{-1} to 3200 cm^{-1}, the total yield $P_{\rm yield}$ and total population $P_{\rm tot}$ decrease rapidly.

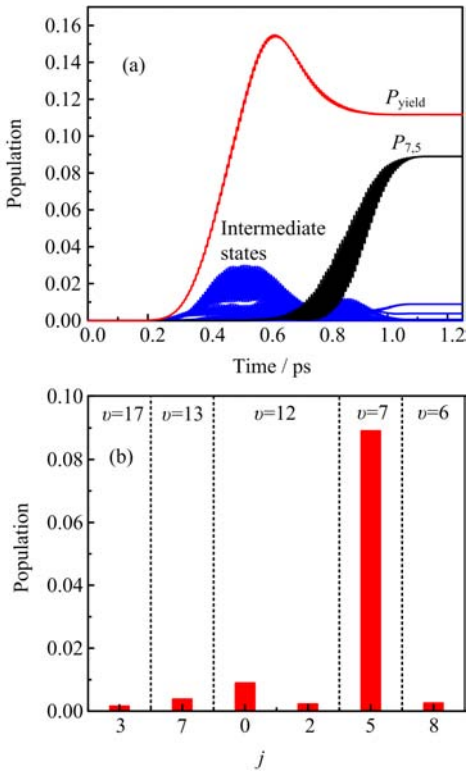

FIG. 6 The population transfer for nine-photon PA reaction. (a) The total yield of associated OH and the populations of the target and intermediate states. (b) The final population distributions at the end of the pulse.

For the nine-photon process we consider here, the initial collision energy E_0 is chosen as 3.01 kJ/mol, and the target state is $|7, 5\rangle$. In this process, the population is transferred to the target state via 19 intermediate sates and 31 transitions, as shown in Fig.5. The optimal carrier frequency and pulse duration are 2114.07 cm^{-1} and 1.161 ps. For the nine-photon scheme, the smaller initial collision energy increases the collision time of the two atoms. So the pulse duration is longer than those for the three- and four-photon schemes.

The population distributions for the nine-photon transition is shown in Fig.6. When the pulse is over, the total yield $P_{\rm yield}$ reaches 11.2%, and about 8.9% of population can be found in the target state $|7, 5\rangle$, as shown in Fig.6(a). It can be seen that the population curves for the total yield and target state appear at ∼0.2 and ∼0.6 ps, respectively. The interval time between these two is longer than those for the above two multi-photon schemes. This indicates that the time for population transfer to target state can be delayed as a multi-photon scheme includes more intermediate states. Moreover, the excessive intermediate states and transitions can increase dissociation probability, which leads to obvious oscillatory behavior in the total yield curve.

Because the pulse frequency is close to the four-photon resonant frequencies for the transitions from

DOI:10.1063/1674-0068/27/05/497-502

continuum state to the sates $|12,0\rangle$ and $|12,2\rangle$, about 1.1% of population stays in these two states, as shown in Fig.6(b). Although the nine-photon scheme includes 31 transitions, most resonant frequencies for these transitions are far from the pulse frequency. When the pulse is over, the population transferred to the intermediate sates is almost zero except the states $|12,0\rangle$ and $|12,2\rangle$. Besides the intermediate states, a small amount of population (0.78%) is transferred to the background states $|17,3\rangle$, $|13,7\rangle$, and $|6,8\rangle$ in Fig.6(b). The state-selectivity for the nine-photon scheme is higher than that for the four-photon scheme.

IV. CONCLUSION

In this work, we studied the rovibrational state-selectivity through multi-photon PA reaction in the ground electronic state, with OH radical as the example. We selected the rovibrational states $|11,1\rangle$, $|10,0\rangle$, and $|7,5\rangle$ as the target states to investigate three-, four-, and nine-photon processes. The calculated results show that the initial collision energy and pulse parameters can determine the transition pathways and control population transferring to different target states. Except for the interested transitions, some other transitions can take place as the pulse frequency is close to these transition frequencies. Therefore, some population can be transferred to the intermediate and background states through these transitions, and the state-selectivity of the target state is decreased. In PA process, a part of associated OH radicals can be dissociated via the intermediate and background states, which decreases the total yield and final population of the target state. To produce OH radicals in a lower rovibrational state, we can see from the three multi-photon schemes that a smaller pulse frequency has to be chosen. This means that multi-photon transition should include more intermediate states and the final population of the target state should be decreased.

V. ACKNOWLEDGMENTS

This work is supported by the National Natural Science Foundation of China (No.11347012).

[1] M. V. Korolkov, G. K. Paramonov, and B. Schmidt, J. Chem. Phys. **105**, 1862 (1996).
[2] S. Thomas , S. Guérin, and H. R. Jauslin, Phys. Rev. A **71**, 013402 (2005).
[3] J. Hu, K. L. Han, and G. Z. He, Phys. Rev. Lett. **95**, 123001 (2005).
[4] M. Tomza, W. Skomorowski, M. Musial, R. Gonzalez-Ferez, C. P. Koch, and R. Moszynski, Mol. Phys. **111**, 1781 (2013).
[5] H. Huanga, Z. H. Luoa, Y. C. Changa, K. C. Laub, and C. Y. Ng, Chin. J. Chem. Phys. **26**, 669 (2013).
[6] N. V. Vitanov and B. W. Shore, Phys. Rev. A **73**, 053402 (2006).
[7] H. T. K. Bergmann and B. W. Shore, Rev. Mod. Phys. **70**, 1003 (1998).
[8] Y. Y. Niu, R. Wang, and M. H. Qiu, Phys. Rev. A **84**, 023406 (2011).
[9] Y. N. Demkov and V. N. Ostrovsky, Phys. Rev. A **61**, 032705 (2000).
[10] T. Hornung, M. Motzkus, and R. de Vivie-Riedle, Phys. Rev. A **65**, 021403(R) (2002).
[11] S. Shi, A. Woody, and H. Rabitz, J. Chem. Phys. **88**, 6870 (1988).
[12] V. Bendkowsky, B. Butscher, J. Nipper, J. P. Shaffer, R. Löw, and T. Pfau, Nature **458**, 1005 (2009).
[13] E. Gomez, A. T. Black, L. D. Turner, E. Tiesinga, and P. D. Lett, Phys. Rev. A **75**, 013420 (2007).
[14] J. M. Sage, S. Sainis, T. Bergeman, and D. DeMille, Phys. Rev. Lett. **94**, 203001 (2005).
[15] I. Manai, R. Horchani, M. Hamamda, A. Fioretti, M. Allegrini, H. Lignier, P. Pillet, and D. Comparat, Mol. Phys. **111**, 1844 (2013).
[16] U. Schlöder, C. Silber, T. Deuschle, and C. Zimmermann, Phys. Rev. A **66**, 061403 (2002).
[17] C. P. Koch, J. P. Palao, R. Kosloff, and F. Masnou-Seeuws, Phys. Rev. A **70**, 013402 (2004).
[18] C. C. Tsai, R. S. Freeland, J. M. Vogels, H. M. J. MBoesten, B. J. Verhaar, and D. J. Heinzen, Phys. Rev. Lett. **79**, 1245 (1997).
[19] B. Schäfer-Bung, R. Mitrić, and V. Bonačić-Koutecký, J. Phys. B **39**, S1043 (2006).
[20] G. K. Paramonov and P. Saalfrank, Phys. Rev. A **79**, 013415 (2009).
[21] E. F. de Lima, T. S. Ho, and H. Rabitz, Chem. Phys. Lett. **501**, 267 (2011).
[22] P. Marquetand and V. Engel, J. Phys. B **41**, 074026 (2008).
[23] Y. Y. Niu, S. M. Wang, and S. L. Cong, Chem. Phys. Lett. **428**, 7 (2006).
[24] M. V. Korolkov, J. Manz, G. K. Paramonov, and B. Schmidt, Chem. Phys. Lett. **260**, 604 (1996).
[25] E. F. de Lima, T. S. Ho, and H. Rabitz, Phys. Rev. A **78**, 063417 (2008).
[26] P. Marquetand and V. Engel, J. Chem. Phys. **127**, 084115 (2007).
[27] R. T. Lawton and M. S. Child, Mol. Phys. **40**, 773 (1980).
[28] E. F. de Lima and J. E. M. Hornos, Chem. Phys. Lett. **433**, 48 (2006).
[29] M. D. Feit, J. A. Jr. Fleck, and A. Steiger, J. Comput. Phys. **47**, 412 (1982).
[30] Y. C. Han, K. J. Yuan, W. H. Hu, T. M. Yan, and S. L. Cong, J. Chem. Phys. **128**, 134303 (2008).
[31] C. C. Marston and G. G. Balint-Kurti, J. Chem. Phys. **91**, 3571 (1989).

DOI:10.1063/1674-0068/27/05/497-502